© 2016. Published by The Company of Biologists Ltd | Journal of Experimental Biology (2016) 219, 470-473 doi:10.1242/jeb.130476

SHORT COMMUNICATION

Hindlimb muscle fibre size and glycogen stores in bank voles with increased aerobic exercise metabolism

Ewa Jaromin*, Julia Wyszkowska, Anna Maria Labecka, Edyta Teresa Sadowska and Paweł Koteja

ABSTRACT

To test hypotheses concerning physiological factors limiting the rate of aerobic exercise metabolism, we used a unique experimental evolution model: lines of bank voles selected for high swim-induced aerobic metabolism (A) and unselected, control lines (C). We investigated putative adaptations that result in the increased performance of the hindlimb muscle (gastrocnemius joined with plantaris). The body mass-adjusted muscle mass was higher in A-lines (0.093 g) than in C-lines (0.083 g; P=0.01). However, selection did not affect mean muscle fibre cross-sectional area (P=0.34) or glycogen content assessed with a histochemical periodic acid–Schiff reaction (PAS; P=0.82). The results suggest that the increased aerobic performance is achieved by an increase of total muscle mass, without major qualitative changes in the muscle fibre architecture. However, such a conclusion should be treated with caution, because other modifications, such as increased density of capillaries or mitochondria, could occur.

KEY WORDS: *Myodes glareolus*, Aerobic capacity, Artificial selection, Fibre types, Gastrocnemius, Locomotor performance

INTRODUCTION

The maximum rate of aerobic exercise metabolism is a trait of special interest from both medical and evolutionary–comparative perspectives, because it is regarded as a reliable index of the overall vital status in humans, and presumably played a crucial role in the evolution of locomotor performance and endothermy (Swallow et al., 2009). Despite intensive research, the discussion concerning physiological factors limiting the rate of aerobic metabolism remains open (Gębczyński and Konarzewski, 2011). To test hypotheses concerning these factors, we used an experimental evolution model: lines of bank voles, *Myodes glareolus* (Schreber 1780), selected for high swim-induced aerobic metabolism (A-lines; Sadowska et al., 2015). In generation 13, voles from the A-lines achieved a 46% higher mass-adjusted aerobic metabolism during voluntary swimming (Fig. S1; Sadowska et al., 2015) and a 20% higher mass-independent maximum rate of oxygen consumption in a forced-exercise test on a treadmill than those from unselected, control C-lines (A. Rudolf, E.T.S. and P.K., unpublished data). We expected correlated changes in subordinate morpho-physiological traits, which should have changed proportionally to the increased performance (Swallow et al., 2009). In the present study, we focused on the putative adaptations in skeletal muscles.

Both endurance training and selection for high aerobic performance result in numerous changes to meet the increased oxygen and substrate demands of working muscles. One of the most profound is shortening the mean distance of diffusive transport of oxygen from capillaries to mitochondria, which can be achieved by decreasing the area of muscle fibres or increasing the number of capillaries (Wong et al., 2009). The increase of sustained aerobic exercise performance can also be facilitated by an increased ratio of the number of slow-twitch oxidative fibres to fast-twitch glycolytic ones (Guderley et al., 2008). For example, it has been shown that endurance training in both humans and rodents results in the transformation of glycolytic fibres into oxidative ones (Yan et al., 2011). The slow oxidative fibres typically contain a lower amount of glycogen than the glycolytic ones (He and Kelley, 2004). Therefore, we hypothesized that selection for high swim-induced aerobic metabolism had resulted in decreased muscle fibre area and decreased fibre glycogen stores (assessed with histochemical periodic acid–Schiff reaction, PAS) in hindlimb muscles.

MATERIALS AND METHODS

The artificial selection experiment

The rationale for and history of the selection experiment on bank voles, and a detailed description of procedures and animal maintenance conditions, are given in Sadowska et al. (2015). In short, A-lines (‘aerobic’) were selected for high aerobic exercise metabolism, measured as the 1 min maximum swim-induced oxygen consumption. Water temperature was maintained at 38°C to ensure that the test involved only locomotor and not thermoregulatory effort. Four replicate A-selected lines and four randomly bred, unselected C-lines (‘control’) were maintained to account for random genetic processes (Fig. S1).

All procedures associated with the breeding scheme, the selection protocol and euthanasia were approved by the Local Bioethical Committee in Krakow, Poland (no. 68/2012).

Histological analyses and muscle fibre measurements

The histological study was performed on 12 adult voles (six males and six females representing different families; note, only five males were used in one of the C-lines) sampled from each of the four A-lines and four C-lines in the 13th experimental generation (95 animals in total). The animals did not undergo a swimming test or any other trials. At the age of 75–79 days (mean 76 days) the individuals were killed by cervical dislocation after isoflurane anaesthesia (Aerrane, Baxter Poland, Warsaw, Poland). Gastrocnemius and plantaris muscles were dissected off and weighed together in order to avoid structure damage during separation of the muscles. Muscles were fixed in 10% buffered neutral formalin, then transferred into 70% ethyl alcohol (line EtOH-B, Linegal Chemicals, Poland) and stored at room temperature until tissue processing and paraffin embedding (Table S1).

Serial 4 µm cross-sections of paraffin-embedded muscle venter were cut with a motorized rotary microtome (Hyrax M55, Zeiss,

Institute of Environmental Sciences, Jagiellonian University, Gronostajowa 7, Krakow 30-387, Poland.

*Author for correspondence (ewa.jaromin@uj.edu.pl)

Received 13 August 2015; Accepted 30 November 2015

Journal of Experimental Biology

Oberkochen, Germany) at one-third and half of the muscle length starting from its origin point at the condyle of the femur. Serial sections were placed on poly L-lysine-coated microscope glass slides and deparaffinized in xylene, then PAS was performed using 1% periodic acid (50 min; Carl Roth, Darmstadt, Germany) and Schiff's reagent (50 min; Carl Roth, Karlsruhe, Germany). Afterwards, slides were cleared in ST Ultra (Leica) and mounted on CV Ultra (Leica).

The cross-sections were pre-examined under a ×10 objective: only intact (not torn), non-folded and properly stained sections were qualified for imaging. Selected cross-sections were scanned under a ×40 objective using the VS120 system (Olympus, Tokyo, Japan), which produces high-resolution multiplane virtual images, examined further in cellSens software (Olympus). To ensure representative sampling of the muscle fibres for analysis, we first divided each cross-section into three compartments that corresponded to the anatomical parts of the hindlimb muscle: internal (including gastrocnemius medial head), central (including plantaris muscle) and external (including gastrocnemius lateral head; Fig. 1A). Each of the three compartments was then divided into arbitrary quarters, one random point was chosen in each of the quarters, and a naturally outlined, cohesive bundle containing the random point was analysed. If the random point indicated a bundle that contained free spaces or was damaged during tissue processing, another bundle, the closest non-damaged one, was chosen for analysis. If the indicated bundle comprised less than 50 fibres, an additional, adjacent bundle was also measured and these bundles were analysed together. The 12 bundles from each cross-section (four in each of the three anatomical compartments) were manually outlined and a circle of similar radius was inscribed in each fibre within the bundle (Fig. 1A,B). The software provided data about the total area of the bundle (μm^2), number of fibres within the bundle and the mean colour saturation of every fibre in the bundle (dimensionless). To exclude cell boundaries from calculation of the saturation, the saturation was measured only for the circles inscribed in the fibres. A reference background saturation (mean saturation in areas where the tissue was not present) was similar in all slides (range: 0.11–0.95) and small in comparison to that of fibre saturation (1.3–132.4), and therefore no correction for background was made. The above analyses were performed by two researchers.

Statistical analyses

Mean fibre area (MA) was calculated by dividing bundle area by the number of fibres within that bundle. Mean fibre colour saturation (MS) was the average saturation of all fibres in a bundle. Therefore, the dependent variables MA and MS were the means for a bundle on a cross-section (12 means for each individual).

First, we analysed the repeatability of measurements performed by the two researchers and homogeneity of the muscle structure across and along its length. On a subset of 16 individuals, separate cross-sections made at half of the muscle length were analysed independently by the two researchers, and a cross-section at one-third of the muscle length was analysed by one of the researchers (each researcher analysed eight of these cross-sections). Pearson correlation coefficients (r) between (a) results obtained independently by the two researchers, (b) results obtained at half and one-third of the muscle length, and (c) results obtained for the three compartments on a cross-section were then calculated.

The main analyses were performed by means of nested ANOVA or ANCOVA mixed models, implemented in SAS version 9.3 (SAS Institute) mixed procedure (with REML estimation method). Body mass was analysed with ANOVA including fixed effects of line type (selected versus control), sex, line type×sex interaction, and random effects of replicate line (nested in line type) and line×sex. Muscle mass was analysed with ANCOVA including the same factors and body mass at dissection as a covariate. For MA the model also included fixed effects of compartment on the cross-section (external versus central versus internal) and line type×compartment, and random line×compartment and block (tissue processing batch) effects. MS was analysed with similar ANOVA models, but instead of body mass, random effects of individual identity (nested in line×sex) and identity×compartment were included, and block variable controlled slide staining batches. Because of their biological or technical relevance, the above effects were retained irrespective of their significance. To improve the distribution of residuals, MA and MS were $\log_{10}$ transformed before the analyses.

Preliminary models for MA or MS also included sex×compartment and line type×sex×compartment interactions. These interactions were not significant and were excluded from the final analysis. Preliminary ANCOVA also included interactions between body mass and the main categorical effects (tests of homogeneity of slopes). The significance of random factors (lines, individuals and their interactions with other factors, and blocks) was tested with a likelihood ratio test. Tukey–Kramer adjustment was used for pairwise *a posteriori* comparisons between compartments.

RESULTS AND DISCUSSION

The analyses performed on a subset of 16 individuals showed that the values of MS were highly correlated between the two cross-sections at half muscle length analysed independently by two researchers ($0.93<r<0.96$, $P<0.001$; Table S2A), between the cross-sections at half and one-third muscle length ($0.74<r<0.93$, $P<0.001$; Table S2B), and between the interior, central and exterior compartments of the same cross-section ($0.67<r<0.95$, $P<0.005$; Table S2C). Similarly, the values of MA (μm^2) were highly correlated between two cross-sections at half muscle length analysed independently by two researchers ($0.82<r<0.94$, $P<0.001$; Table S2A) and the cross-sections at half and one-third muscle length ($0.74<r<0.85$, $P<0.001$; Table S2B). However, the correlations between MA measured on three compartments of the same cross-section were usually lower ($0.48<r<0.79$, $P<0.06$; Table S2C). Thus, the muscle venter was morphologically more differentiated (in terms of fibre size) across a cross-section than along its length. Therefore, we decided to perform all further measurements on only one cross-section (at half of its length), but on more fibre bundles at this location, rather than on fewer bundles on two cross-sections. The high correlation between results obtained independently by the two researchers showed that the method of choosing the bundles of fibres for analyses provided a representative sample and that the estimates of MA and MS were highly repeatable.

Body mass was higher in males than in females ($P<0.01$), but did not differ significantly between A- and C-lines ($P=0.81$) and the line type×sex interaction was not significant (Table 1). Combined gastrocnemius and plantaris muscle mass increased with body mass [common slope with 95% confidence limits (CL): 0.0025 (0.0019–0.0031) g g^{-1}, $t_{78}=8.49$, $P<0.001$]. The muscle mass, adjusted for body mass, was higher in males than in females and higher in A-lines than in C-lines (the line type×sex interaction was not significant; Table 1). A likelihood ratio test indicated that random replicate line effect contributed significantly to the muscle mass variance ($\chi^2=6.5$, $P=0.011$).

MA (log transformed) increased with body mass in both A- and C-lines [common slope (95% CL): 0.003 (0.001–0.005) log(μm^2) g^{-1}, $t_{1104}=3.34$, $P<0.001$]. Mass-adjusted MA did not

Journal of Experimental Biology (2016) 219, 470-473 doi:10.1242/jeb.130476

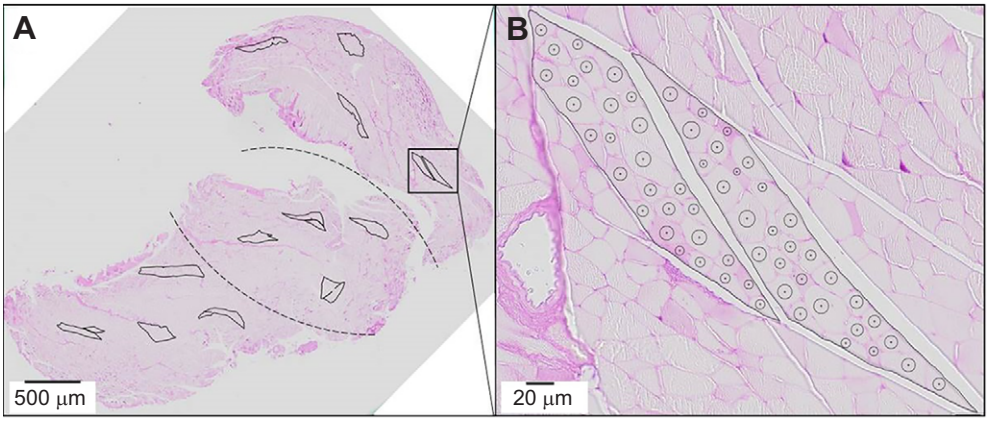

Fig. 1. Periodic acid–Schiff-stained cross-section of a bank vole's hindlimb muscle. (A) The division into three compartments, which approximately correspond to the anatomical sections of the hindlimb muscle, is shown by the dashed lines: external (including lateral gastrocnemius head), central (including plantaris muscle and part of gastrocnemius muscle) and internal (including medial gastrocnemius head). Measurement bundles are outlined with solid lines; the software provided the area of the outlined shapes. (B) Different shades of pink indicate indirectly the glycogen content in the muscle fibre. The software provided data about mean colour saturation of every circle inscribed in a single fibre.

differ significantly between the A- and C-lines or between sexes (Table 1). We expected that selection would differently modify the three muscle compartments (Guderley et al., 2008), but neither the effect of compartment nor the line type×compartment interaction was significant (Table 1). The line type×sex interaction was not significant either. In the above analysis, we assumed a common regression slope, even though body mass×sex and body mass×sex×line type interactions were marginally significant (both P=0.04). Therefore, we also performed the analysis separately for males and females, but the additional results did not change the conclusions (Table S3). Random effects contributed significantly to the variance of MA (replicate lines: χ^2=32.3, P=0.000; line×compartment: χ^2=4.7, P=0.03; line×sex: χ^2=4.2, P=0.04; and tissue processing block: χ^2=5.8, P=0.016).

Mean fibre PAS staining saturation (MS; log transformed), the index of glycogen content, tended to be higher in males than in

Table 1. Body mass and hindlimb muscle mass, mean fibre area and glycogen content index in bank voles from the selected (*N*=48) and control (*N*=47) lines

Dependent variable	Fixed factor	Factor level	LSM (95% CL)	*F*-statistic ($d.f._N$, $d.f._D$)	*P*-value
Body mass (g)	Line type	Selected	22.5 (21.0–24.0)	0.06 (1,6)	0.81
		Control	22.3 (20.7–23.8)		
	Sex	Female	20.6 (19.1–22.1)	18.1 (1,6)	0.01
		Male	24.1 (22.7–25.6)		
	Line type×sex			1.61 (1,6)	0.25
Muscle mass (g)	Line type	Selected	0.093 (0.088–0.098)	11.7 (1,6)	0.01
		Control	0.083 (0.077–0.088)		
	Sex	Female	0.084 (0.079–0.088)	16.5 (1,6)	0.01
		Male	0.092 (0.088–0.097)		
	Line type×sex			0.04 (1,6)	0.85
Mean fibre area (μm^2)	Line type	Selected	404 (346–471)	1.09 (1,6)	0.34
		Control	389 (334–455)		
	Compartment	External	408 (356–467)	2.18 (2,12)	0.16
		Central	392 (342–449)		
		Internal	390 (341–447)		
	Sex	Female	390 (335–454)	1.98 (1,6)	0.21
		Male	403 (347–469)		
	Line type×sex			3.39 (1,6)	0.12
	Line type×compartment			0.57(2,12)	0.58
Mean saturation of PAS staining	Line type	Selected	17.2 (13.2–22.5)	0.06 (1,6)	0.82
		Control	16.7 (12.7–21.8)		
	Compartment	External	17.2 (14.1–21.0)	4.67 (2,12)	0.03
		Central	15.9 (13.1–19.4)		
		Internal	17.7 (14.6–21.6)		
	Sex	Female	15.1 (11.8–19.4)	5.07 (1,6)	0.06
		Male	18.9 (14.8–24.3)		
	Line type×sex			0.05 (1,6)	0.84
	Line type×compartment			1.37 (2,12)	0.29

Muscle mass is gastrocnemius plus plantaris muscle mass. Mean saturation of PAS staining (dimensionless) provides an index of glycogen content. The results are presented as back-transformed least square means (LSM) with 95% confidence limits (CL) from mixed ANOVA/ANCOVA models. $d.f._N$, nominator degrees of freedom; $d.f._D$, denominator degrees of freedom.

Journal of Experimental Biology

females (P=0.06), but did not differ between line type (P=0.82; Table 1). MS was significantly lower in the central than in the internal compartment (*post hoc* Tukey test: t_{12}=2.96, P=0.03; Table 1), and intermediate in the external one (central versus external: t_{12}=2.13, P=0.12; external versus internal: t_{12}=0.83, P=0.69). The line type×compartment and sex×compartment interactions were not significant (Table 1). Some of the random effects contributed significantly to the variance of MS (replicate lines: χ^2=2.5, P=0.114; line×compartment: χ^2=29.6, P=0.000; line×sex: χ^2=1.9, P=0.168; individual identity: χ^2=743.2, P=0.000; and identity×compartment: χ^2=25.4, P=0.000).

According to the 'optimal fibre size hypothesis', actual fibre size should be a compromise between small fibres that shorten oxygen diffusion distance and large fibres, for which membrane potential costs are lower because of a lower surface area to volume ratio (Jimenez et al., 2013). Decreased fibre area shortens diffusion distance, so it can be an adaptation to higher aerobic performance. Indeed, Wong et al. (2009) showed that selection for high voluntary wheel-running in laboratory mice, i.e. a trait associated with aerobic locomotor performance, resulted in decreased muscle mass and decreased fibre area. In another experimental evolution model system, selection for high endurance running in rats resulted in similar changes (decreased muscle mass and fibre area; Howlett et al., 2003). Our results indicate that selection for high aerobic performance does not necessarily result in alterations in muscle fibre area.

Slow-twitch oxidative fibres, characterized by lower glycogen content than fast-twitch glycolytic ones, are widely recognized to play a major role in endurance physical performance. Yet, PAS staining revealed no differences in the glycogen content of the muscle fibres between voles from the A- and C-lines. Similarly, rats selected for high endurance running did not have an increased percentage of oxidative fibres or changed glycogen content compared with those selected for low endurance running (Howlett et al., 2003). However, selection for high wheel-running performance in mice resulted in an increased proportion of oxidative fibres (Guderley et al., 2008) and simultaneously a higher glycogen content when compared with unselected mice (Gomes et al., 2009). Therefore, based only on the PAS staining results, modifications to muscle fibre-type composition in our model system cannot definitely be excluded.

It could be argued that the effect of selection on the muscle fibre characteristics was not detected because the samples of fibres analysed were not representative for a muscle. However, we showed that the results obtained independently by two researchers, and results for cross-sections from two distant sites of the muscles, were highly correlated. Moreover, the analyses revealed significant random effects of replicate lines. Therefore, the methodology was also adequate to detect a difference between the A- and C-lines if it was greater than expected from random effects.

To summarize, our results suggest that the increased aerobic performance of muscles from the selected voles was achieved mainly by an increase in muscle mass, without major qualitative changes in the muscle architecture. However, such a conclusion should be treated with caution, because other modifications, such as increased density of capillaries or mitochondria, could occur. Such possibilities, as well as possible modifications in the central oxygen delivery systems (pulmonary and cardiovascular), will be the subject of further research within the framework of our unique experimental evolution model system.

Acknowledgements
We thank Dagmara Filak and Magdalena Guńska for performing tissue dissections. We thank the many technicians and students, especially K. Baliga-Klimczyk, K. Chrząścik, G. Dheyongera, A. Rudolf, C. Stawski, B. Bober-Sowa, J. Hajduk, I. Nowak, K. Sęk and K. Ścigajło, who contributed to animal maintenance and selection protocols.

Competing interests
The authors declare no competing or financial interests.

Author contributions
P.K., E.T.S. and A.M.L. conceived and organized the study; E.J. and J.W. performed the histological analyses; E.J., E.T.S. and P.K. analysed the data and interpreted the results; E.J. and J.W. wrote the draft manuscript and all co-authors participated in editing the final version.

Funding
The study was supported by the National Science Centre in Poland [DEC-2011/03/B/NZ4/02152 to P.K.]; and the Jagiellonian University [DS/WBINOZ/INOS/757 to P.K.].

Supplementary information
Supplementary information available online at
http://jeb.biologists.org/lookup/suppl/doi:10.1242/jeb.130476/-/DC1

References
Gębczyński, A. K. and Konarzewski, M. (2011). Effects of oxygen availability on maximum aerobic performance in *Mus musculus* selected for basal metabolic rate or aerobic capacity. *J. Exp. Biol.* **214**, 1714-1720.

Gomes, F. R., Rezende, E. L., Malisch, J. L., Lee, S. K., Rivas, D. A., Kelly, S. A., Lytle, C., Yaspelkis, B. B. and Garland, T. (2009). Glycogen storage and muscle glucose transporters (GLUT-4) of mice selectively bred for high voluntary wheel running. *J. Exp. Biol.* **212**, 238-248.

Guderley, H., Joanisse, D. R., Mokas, S., Bilodeau, G. M. and Garland, T. (2008). Altered fibre types in gastrocnemius muscle of high wheel-running selected mice with mini-muscle phenotype. *Comp. Biochem. Physiol. B Biochem. Mol. Biol.* **149**, 490-500.

He, J. and Kelley, D. E. (2004). Muscle glycogen content in type 2 diabetes mellitus. *Am. J. Physiol. Endocrinol. Metab.* **287**, E1002-E1007.

Howlett, R. A., Gonzalez, N. C., Wagner, H. E., Fu, Z., Britton, S. L., Koch, L. G. and Wagner, P. D. (2003). Selected Contribution: skeletal muscle capillarity and enzyme activity in rats selectively bred for running endurance. *J. Appl. Physiol.* **94**, 1682-1688.

Jimenez, A. G., Dillaman, R. M. and Kinsey, S. T. (2013). Large fibre size in skeletal muscle is metabolically advantageous. *Nat. Commun.* **4**, 2150.

Sadowska, E. T., Stawski, C., Baliga-Klimczyk, K., Chrząścik, K. M., Dheyongera, G., Rudolf, A. and Koteja, P. (2015). Evolution of basal metabolic rate in bank voles from a multidirectional selection experiment. *Proc. R. Soc. B. Biol. Sci.* **282**, 20150025.

Swallow, J. G., Hayes, J. P., Koteja, P. and Garland, T. (2009). Selection experiments and experimental evolution of performance and physiology. In *Experimental Evolution: Concepts, Methods, and Applications of Selection Experiments* (ed. T. Garland and R. R. Rose), pp. 320-370. Berkeley: University of California Press Ltd.

Wong, L. E., Garland, T., Rowan, S. L. and Hepple, R. T. (2009). Anatomic capillarization is elevated in the medial gastrocnemius muscle of mighty mini mice. *J. Appl. Physiol.* **106**, 1660-1667.

Yan, Z., Okutsu, M., Akhtar, Y. N. and Lira, V. A. (2011). Regulation of exercise-induced fiber type transformation, mitochondrial biogenesis, and angiogenesis in skeletal muscle. *J. Appl. Physiol.* **110**, 264-274.